PROCEEDINGS, TOUGH Symposium 2012
Lawrence Berkeley National Laboratory, Berkeley, California, September 17-19, 2012

SIMULATING MICROHOLE-BASED HEAT MINING FROM ENHANCED GEOTHERMAL SYSTEMS

Yingqi Zhang[a], Lehua Pan[a], Patrick Dobson[a], Ken Oglesby[b], Stefan Finsterle[a]

[a] Lawrence Berkeley National Laboratory
Earth Sciences Division, MS 74-120
Berkeley, CA, 94708
e-mail: YQZhang@lbl.gov

[b] Impact Technologies, LLC
Tulsa, Oklahoma 74153

ABSTRACT

This study investigates the use of microholes as a potential approach to enhancing fluid flow and heat exchange within an engineered geothermal system (EGS), using numerical simulations. The idea behind microholes is that injecting the working fluid into a large number of spatially distributed microholes, rather than a few conventionally drilled wells, is likely to provide access to a larger reservoir volume, with enhanced overall flow distances and increased contact area between flowing fractures and the hot rock matrix. In this paper, we compare heat recovery factors calculated for EGS reservoirs with a conventional well configuration and with microhole arrays. The synthetic reservoir used has properties similar to those of the EGS test site at Soultz-sous-Forêts. The simulations provide preliminary insights into the potential of microholes for improving the efficiency and robustness of heat extraction from an EGS.

INTRODUCTION

In addition to a heat source, extraction of geothermal energy requires fluids that are able to transfer the heat from the hot rock matrix to the surface, and interconnected pore space that allows fluid flow at an appropriate rate between injection and production wells. In the absence of such favorable conditions, the concept of enhanced geothermal systems (EGS) provides a means to create a reservoir by hydraulically or thermally fracturing the rock to generate or increase permeability and inter-well connectivity, allowing injected working fluids to pick up reservoir heat as they flow along the created permeable pathways toward production wells.

Advances in drilling technology are essential for the technical success and economic viability of EGS. Specifically, the development of drilling technology for slimholes or microholes (bores less than 4 inches or 10.2 cm diameter) (Pritchett, 1998; Finger et al., 1999) may offer the flexibility needed to design well configurations that enable optimization of geothermal heat mining using EGS.

The objective of this study is to examine the potential of microholes—used as injection or production wells—to improve the efficiency and sustainability of geothermal energy production, as compared to EGS with a conventional well configuration. We test the supposition that this improved performance is achieved because (1) directionally drilled microholes can be distributed widely (both horizontally and vertically), so they intersect a larger portion of the hot reservoir and its fracture network, thus increasing the rock volume that is accessed by the circulating working fluid; and (2) the distributed nature of flow originating from or converging to spatially separated microholes reduces the risk of creating thermal short circuits.

These premises are examined through numerical modeling of a synthetic EGS reservoir, which is modeled after (but does not represent) the conditions at the European EGS test site at Soultz-sous-Forêts, France (e.g., Gérard and Kappelmeyer, 1987; Sausse et al., 2010). Temperatures and recovery factors are calculated for a conventional well configuration and one based on microhole arrays.

MODEL DEVELOPMENT

Reservoir Model

The reservoir model developed for the comparison of EGS performance using conventional and microhole well configurations has characteristics similar to those encountered at the European EGS demonstration site in Soultz-sous-Forêts, France. However, this is strictly a synthetic modeling study, and no conclusions about the potential performance of microholes at the test site should be drawn from this analysis, as the model is a highly simplified representation of the conditions at Soultz-sous-Forêts.

The model domain consists of a rectangular cuboid of dimensions 2.0 × 3.0 × 1.5 km, positioned at a depth between 3.8 and 5.3 km. The temperatures at the impermeable top and bottom boundaries of the model domain are fixed at 160ºC and 200ºC, respectively. Initial pressures vary hydrostatically from about 3.7 MPa at the top to about 5.1 MPa at the base. Within this block of low-permeability rock lies the EGS reservoir, consisting of a zone of fractures that were created or reactivated by hydraulic stimulation. The shape and size of this zone is based on the cloud of micro-seismic events recorded at Soultz-sous-Forêts (Michelet and Toksöz, 2007); the zone is assumed to be a horizontal, approximately elliptical region with a length and width of about 2.0 km and 1.0 km, respectively, and a thickness of 0.4 km, located at a depth between 4.4 and 4.8 km. The EGS reservoir is represented by a dual-permeability model, where permeable fractures and the essentially impermeable rock matrix are modeled as overlapping interacting continua. We account for global heat flow through the matrix continuum added to global fracture flow and the interaction between the fracture and matrix continua.

Finally, within the fractured EGS reservoir, we added a highly permeable, planar wide-aperture feature as a potential zone for preferential flow between the injection and production wells. We define the slightly inclined plane by the points of highest injectivity observed during hydraulic testing at Soultz-sous-Forêts (Sausse et al., 2010); it is assumed to extend across the entire stimulated reservoir.

The key heat mining process can be described as conductive heat transfer between the hot rock matrix and the working fluid flowing through the fracture network; this sustains the convective transport of heated fluid to the production well. The overall effectiveness of the conductive heat transfer depends on the contact area between the rock and the working fluid, which as a first approximation can be taken as the total fracture surface area. However, flow is likely to be channelized, i.e., the actual contact area available for heat transfer is substantially smaller than the geometric fracture surface area, which is calculated from fracture spacing information for the dual-permeability model. We therefore include a contact area reduction factor and apply it to the dual-permeability regions of our model. Table 1 summarizes some key model parameters.

Table 1. Base-case model parameters and ranges examined in global sensitivity analysis

Parameter	Value
Log_{10}(permeability wide-aperture zone [m^2])	-10.0
Log_{10}(permeability fractures horizontal [m^2])	-13.0
Log_{10}(permeability fractures vertical [m^2])	-13.0
Log_{10}(permeability matrix [m^2])	-18.0
Porosity wide-aperture zone [%]	2.0
Porosity fractures [%]	0.5
Porosity matrix [%]	5.0
Fracture spacing [m]	30.0
Log_{10}(fracture-matrix area reduction [-])	-1.0
Thermal conductivity [W m^{-1} ºC^{-1}]	3.0
Heat capacity [J kg^{-1} ºC^{-1}]	950.0
Injection rate [kg s^{-1}]	80.0
Injection temperature [ºC]	50.0

EGS performance is simulated using the non-isothermal, multiphase, multicomponent flow and transport code TOUGH2 (Pruess et al., 1999; http://esd.lbl.gov/TOUGH), as incorporated into iTOUGH2 (Finsterle, 2004; http://esd.lbl.gov/iTOUGH2).

Well Configurations

We compare EGS heat mining performance using two distinct well configurations (Fig. 1). The first configuration consists of conventionally drilled, large-diameter injection and production wells in an arrangement similar to that used at Soultz-sous-Forêts (Fig. 1a), where three conventional wells, aligned parallel to the maximum principal stress, were drilled from a single well pad, reaching the target formation at a depth between 4.5 and 5.0 km, and having a bottomhole separation distance of about 600 m. Cold water is injected through the central well, and hot water is produced from the two peripheral wells.

In the second configuration (Fig. 1b), 40 microholes of diameter 0.064 m emanate as two arrays from a conventionally drilled well. Thirty-four of the 40 microholes are drilled such that their end points circumscribe the outer edge of the stimulated zone, with the remaining six microholes terminating on the short axis of the elliptical fracture zone (i.e., the pattern of the end points of the microhole arrays resembles the Greek character θ). The kickoff angle of the microholes is 45º from the axis of the central well. While most likely curved in a real application, we assume that they are drilled straight until they reach their final position in the X-Y plane, at which point they become vertical. Each microhole is approximately 1 km long. The first array of 13 microholes kicks off at a depth of 3.8 km; this array comprises the microholes that reach the outermost portion of the EGS reservoir. The second array consists of the remaining 27 microholes, which emanate from the conventional well at a depth of 4.1 km. The microholes are used for injection; two conventional wells are used for production. The conventional wells are the same as those shown in Fig. 1a, except that the central well is shorter, terminating at the lowest microhole kickoff point at a depth of 4.1 km.

The conventional wells and the microholes are explicitly discretized in our numerical model, albeit in a simplified manner. Following the trajectory of the borehole, cylindrical gridblocks are inserted into the existing elements of the basic grid (Fig. 1a shows the basic grid on the faces of the model domain, where the unstructured, elliptical part indicates the location of the EGS reservoir). These well elements are connected to each other in the axial direction and to the elements in which they are embedded. The conventional wells are perforated only within the stimulated reservoir zone; the microholes are uncased and thus connected to the formation over their entire length.

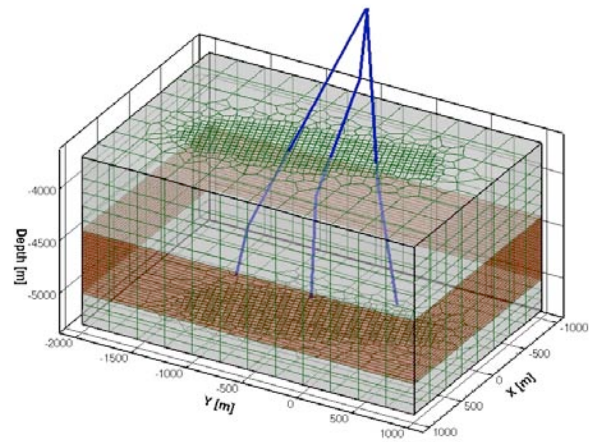

(a)

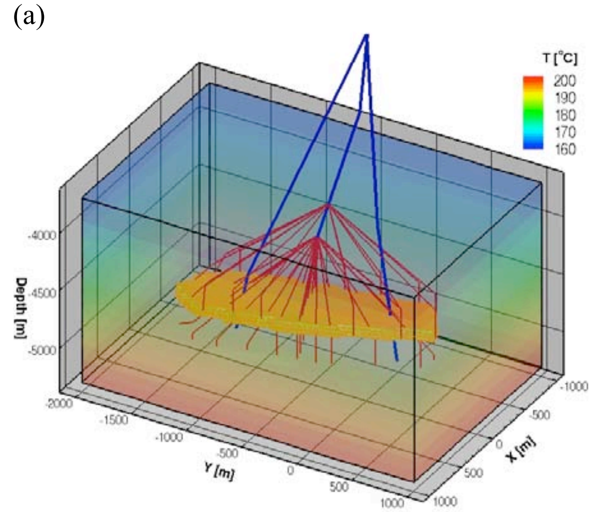

(b)

Figure 1. Simulated borehole configurations: (a) conventional wells, numerical grid on model domain faces, with unstructured portion indicating projection of elliptical EGS reservoir (model layer containing reservoir is highlighted); (b) microhole arrays, initial temperature distribution, and wide-aperture zone

Wellbore flow is calculated using the standard Darcy law with an effective permeability, which was determined for the expected flow velocities using a wellbore simulator that is integrated into the TOUGH2 code, calculating the transient multiphase nonisothermal wellbore flow using the drift-flux model (Pan et al., 2011). For the wellbore sections above the model domain, i.e., from the land surface to a depth of 3,800 m, a semi-analytical solution for radial heat exchange with the surrounding formation is used (Zhang et al., 2011) to efficiently calculate heating of the injected water and heat losses from the produced water. Given the relatively long vertical flow distance in these wellbore sections, gravitational potential is added to the energy balance equation (Stauffer et al., 2003).

Heat Recovery Factor

The comparison of conventional and microhole-based EGS is made using a simple performance measure, which is the heat recovery factor at the end of a 30-year exploitation period. The heat recovery factor is defined as the cumulative heat recovered at the well head divided by the initial heat in the reservoir, E_0:

$$F = \frac{\int (q_p h_p - q_i h_i)\, dt}{E_0} = \frac{\Delta E}{E_0} \tag{1}$$

Here, q_p and q_i are the mass production and injection rates, and h_p and h_i are the enthalpies of the produced and injected fluids, respectively. The net energy extracted from the reservoir, ΔE, can be used to assess the electrical potential of the well system. In addition to the heat recovery factor as an integral performance measure, we also monitor the thermal drawdown in the production wells as a function of time.

RESULTS AND DISCUSSION

We first describe the temperature of the produced fluid and the total thermal energy extracted from the two wells for an exploitation period of 30 years. Both configurations—injection through a conventional, central well and injection through an array of microholes—are presented and compared. Fig. 2 shows the temperature evolution of the produced fluid, which is indicative of thermal breakthrough and overall heat mining effectiveness.

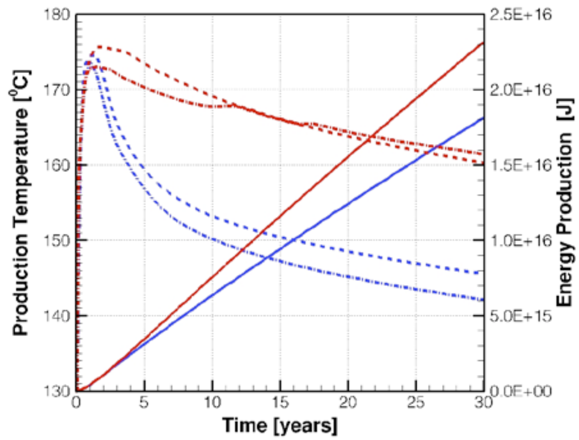

Figure 2. Fluid temperatures at well head of left (dash-dotted lines) and right (dashed lines) production wells for conventional (blue) and microhole (red) configurations. Total produced thermal energy (solid lines).

The temperature of the produced fluid at very early times is essentially equal to the temperature encountered at the depth of the wide-aperture, high-permeability feature, which is the main feed zone. Temperatures at the well head rise as the relatively colder fluid that is initially in the wells is flushed out, and as the formation in the immediate vicinity of the production wells warms up, reducing heat losses in the upper part of the reservoir and in the 4 km long sections from the reservoir to the surface, as calculated using the semi-analytical approach of Zhang et al. (2011).

After this initial temperature increase, colder injection fluid soon reaches the production wells, leading to substantial cooling, especially for the conventional well configuration. The temperatures in the two production wells differ slightly as the feed zones are at different depths due to the inclination of the wide-aperture zone, and due to the fact that their location with respect to the injection well and the geological features are asymmetric. In contrast to the conventional well case, injection through a microhole array distributes the fluid over a wider volume of the stimulated reservoir. Flow velocities in the formation are slower, and a larger fraction of the produced water enters the well through the fracture network of the stimulated rock rather than almost exclusively through the wide-aperture feed zones, as is the case for the conventional well configuration. As a result, thermal breakthrough is much less pronounced, and the temperature of the produced fluids at the end of the simulated period is substantially higher (approximately 161°C) compared to that obtained with the conventional well configuration (approximately 146°C).

Fig. 2 also shows the cumulative heat extracted from the reservoir, which mirrors the trend of the production temperature as the total flow rate remains essentially constant and (for this system which is essentially closed for fluid flow, but not for heat flow) equal to the injection rate of 80 kg/s. For the base-case scenario, about 27% more energy is produced with the microhole configuration.

Fig. 3 shows the temperature distribution after 30 years of exploitation for both the conventional and microhole configurations. The conventional well configuration results in a large volume of fluid flowing along the wide-aperture zone, limiting heat exchange to a relatively narrow channel. This is clearly visible as an essentially one-dimensional zone of reduced temperature between the injection and production wells. In contrast, injecting the working fluid through a microhole array accesses a larger reservoir volume from which heat can be extracted. The temperature decline in that region, which includes a substantial portion of the fractured reservoir outside the wide-aperture zone, is proportionally less severe; this is reflected in the higher temperature of the produced fluid (see Fig. 2).

These simulations support the concept that distributing the working fluid through microholes leads to more effective heat extraction from a larger rock volume, and is less susceptible to the presence of a wide-aperture feature that promotes preferential flow, reduced contact with the reservoir matrix, and thus early thermal breakthrough. Note that the configuration of the microhole array (the number of microholes, their length, diameter, orientation, and spatial distribution) has not been optimized for maximum heat mining efficiency. It has been designed based on simple criteria assuming some knowledge about the extent of the stimulated reservoir. A formal optimization of microhole configuration parameters to maximize heat recovery factors will be undertaken in a future analysis.

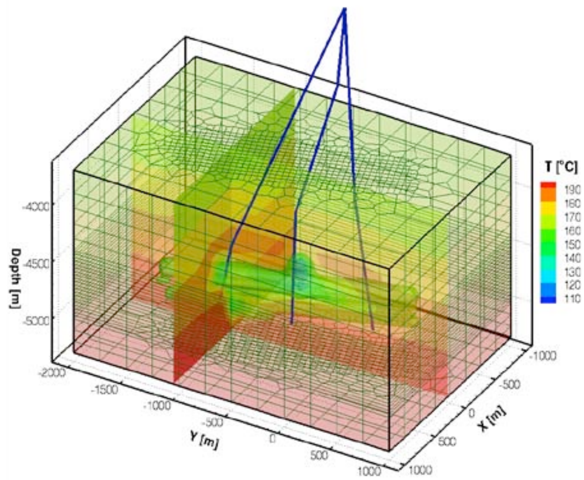

(a)

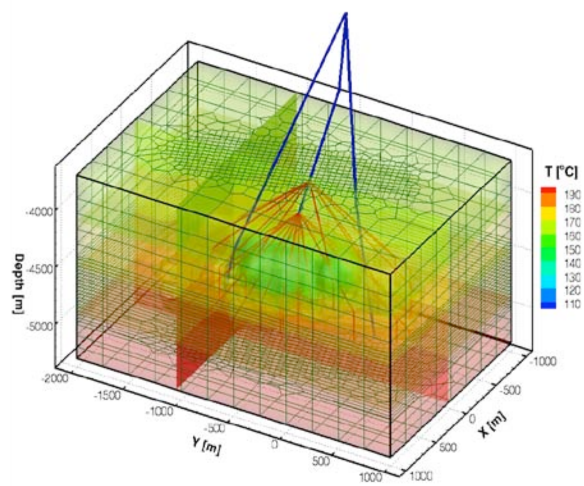

(b)

Figure 3. Simulated temperature distribution after 30 years of exploitation using (a) conventional and (b) microhole configurations.

CONCLUDING REMARKS

The success and sustainability of energy production from enhanced geothermal systems largely depends on the ability of the working fluid to get in contact with a substantial volume of hot reservoir rock. Large-scale stimulation of existing fractures or creation of a new fracture system with sufficient density and connectivity is a prerequisite. However, even if such stimulation is successful, the volume of the heat-storing reservoir accessed by the working fluid may be

very limited for a conventional well configuration, where cold water is injected at discrete locations within a small number of injection wells and produced from a few feed zones in production wells.
The flexibility offered by microhole drilling technology enables installation of a large number of boreholes from a central well, in a configuration that allows for distributed injection (or production) of geothermal working fluids. Such a configuration has the potential to (1) increase the probability of intersecting flowing fractures, (2) increase the fracture surface area contacted by circulating water and thus increase the volume of rock accessible for heat mining, and (3) reduce the risk of flow channeling and early thermal breakthrough.

The generic modeling study presented here indicates that EGS based on microhole arrays could significantly increase heat mining rates and their sustainability over longer time periods.

While the study examined the general concept and showed the potential benefits of microhole-based EGS, its viability strongly depends on the technical feasibility and costs of drilling microhole arrays from a central, conventionally drilled large-diameter well. Great advances have been made in horizontal and directional drilling, opening up opportunities for additional well configurations that support the overall goal of increasing the accessible rock volume. Stimulation of that rock volume is another key issue that may benefit from the flexibility offered by advanced drilling technologies and multiple wells emplaced with an optimized configuration. Some of these issues will be addressed in future research.

ACKNOWLEDGMENT

This work was supported by Lawrence Berkeley National Laboratory under U.S. Department of Energy, Assistant Secretary for Energy Efficiency and Renewable Energy, Geothermal Technologies Program, Contract No. DE-FOA-0000075: Recovery Act: Enhanced Geothermal Systems Component Research and Development/Analysis.

REFERENCES

Finger, J., R. Jacobson, C. Hickox, J. Combs, G. Polk, and C. Goranson, *Slimhole Handbook: Procedures and Recommendations for Slimhole Drilling and Testing in Geothermal Exploration*, Report SAND99-1076, Sandia National Laboratories, Albuquerque, New Mexico, 1999.

Finsterle, S., Multiphase inversion modeling: Review and iTOUGH2 applications, *Vadose Zone Journal*, *3*, 747–762, 2004.

Gérard, A., and O. Kappelmeyer, The Soultz-sous-Forêts project, *Geothermics, 16*(4), 393–399, 1987.

Michelet, S., and M.N. Toksöz, Fracture mapping in the Soultz-sous-Forêts geothermal field using microearthquake locations, *Journal of Geophysical Research*, *112*, B07315, 2007.

Pan, L., C.M. Oldenburg, K. Pruess, and Y.S. Wu, Transient CO_2 leakage and injection in wellbore-reservoir systems for geologic carbon sequestration, *Greenhouse Gases: Science and Technology, 1*(4), 335–350, 2011.

Pritchett, J.W., *Electrical Generating Capacities of Geothermal Slim Holes*, Report MTSD-DFR-98-16223, Maxwell Technologies Systems Division, Inc., San Diego, California, 1998.

Pruess, K., C. Oldenburg, and G. Moridis, *TOUGH2 User's Guide, Version 2.0*, Report LBNL-43134, Lawrence Berkeley National Laboratory, Berkeley, Calif., 1999.

Sausse, J., C. Dezayes, L. Dorbath, A. Genter, and J. Place, 3D model of fracture zones at Soultz-sous-Forêts based on geological data, image logs, induced microseismicity and vertical seismic profiles, *C. R. Geoscience,* 342, 531–545, 2010.

Stauffer, P.H., J.S. Stein, and B.J. Travis, *The Correct Form of the Energy Balance for Fully Coupled Thermodynamics in Liquid Water*, Report LA-UR-03-1555, Los Alamos National Laboratory, Los Alamos, New Mexico, 2003.

Zhang, Y., L. Pan, K. Pruess, and S. Finsterle, A time-convolution approach for modeling heat exchange between a wellbore and surrounding formation, *Geothermics*, *40*(4), 251–266, 2011.